

# In Vivo Blood Characterization from Bioimpedance Spectroscopy of Blood Pooling

Tao Dai

*Department of System and  
Computer Engineering (SCE),  
University of Carleton,  
Canada*

e-mail: tdai@sce.carleton.ca

Andy Adler

*Department of System and  
Computer Engineering (SCE),  
University of Carleton,  
Canada*

e-mail: adler@sce.carleton.ca

## Abstract

Characterization of blood impedance properties is important to estimate clinical diagnostic indices such as haematocrit, glucose level and hydration. Current *in vivo* bioimpedance spectroscopy methods are performed on a body appendage and thus represent a combined measurement of all tissues in the measurement field, rather than the blood individually. This paper describes a novel *in vivo* measurement technique to calculate bioelectrical properties of blood while excluding the disturbances from surrounding tissues, based on analysis of the impedance changes caused by blood accumulation. The forearm was modelled as a cylinder containing anatomical structures such as skin-fat layer, muscles, bones. Blood volume was modeled as the inner cylinder. A tetrapolar electrode system was applied to a human forearm and the impedance curves measured with and without blood pooling were processed to calculate the impedance parameters of arterial blood. The bioelectrical parameters of blood were estimated by fitting the blood curve to a Cole-Cole model using the Levenberg-Marquardt (LM) nonlinear curve fitting method. The approach proposed was verified using an experimental phantom, an equivalent circuit model and a preliminary human experiment. Results show that electrical properties of blood and surrounding tissues can be separated successfully. Of Cole-Cole parameters, the characteristic frequency  $f_c$  is the most reliable parameter to characterize blood bioelectrical properties. This method may allow simplified measurement of blood characteristic parameters for many biomedical and clinical monitoring applications.

## Index Terms

Bioimpedance spectroscopy, Blood pooling, Cole-Cole model, Nonlinear curve fitting, Impedance plethysmography.

## I. INTRODUCTION

THE bioimpedance measurements on humans have seen significant interest because of several advantages, such as low cost, ease of application, non-invasiveness and capability for on-line monitoring [1] [2]. The original bioimpedance technique was *bioelectrical impedance analysis* (BIA). Within a decade, this technique evolved into the more advanced technique known as *bioelectrical impedance spectroscopy* (BIS), also called *multiple-frequency bioimpedance analysis* (MFBIA). BIS applies multi-frequency stimulations to measure body impedance, and has been used for applications such as: body fluid measurement [3] [4] which estimates extracellular fluid (ECF), intracellular fluid (ICF) and total body water (TBW); tissue volume change, such as the impedance plethysmography [5]; and tissue characterization which is mostly based on Cole-Cole model parameters [6]: for example, normal and ischemic tissues were differentiated by comparing  $R_0$  and  $f_c$  [7]; plasma resistance, intracellular resistance and cell membrane capacitance of blood were calculated using three measuring frequencies [8]. Characterization of blood bioimpedance properties is of importance for the development of methods estimating some clinical diagnostic indices such as haematocrit, glucose level and hydration. However, current bioimpedance spectroscopy measurements of blood are either *in vitro* [8] [9] or are performed on a body appendage and thus represent a combined measurement of all tissues in the measuring field [10], rather than the blood impedance value. In this paper, we propose an *in vivo* measurement strategy to calculate bioelectrical properties of arterial blood based on the pulsatile bioimpedance signal in a finger. This work extends our previous conference publication [11].

Blood pooling methods were adopted to measure the fluid and blood volume change of the abdomen, thigh, and calf of aircraft pilots [21] [12]. This method occludes veins to prevent blood flowing out of the segment being investigated.

In this paper, we propose a novel scheme to measure blood impedance *in vivo* by analyzing the difference of bioimpedance spectroscopies before and after blood pooling. By using this method, blood parameters can be separated from those of the surrounding tissues.

## II. METHODS

We consider a tetrapolar impedance sensor applied to the human forearm so that an alternating current enters the forearm from two injection electrodes and the voltage is measured between two measurement electrodes. The physiological structure of this compartment is relatively simple compared with other measuring sites (*e.g.*, chest) and can be approximated with a cylindrical model (Figure 1).

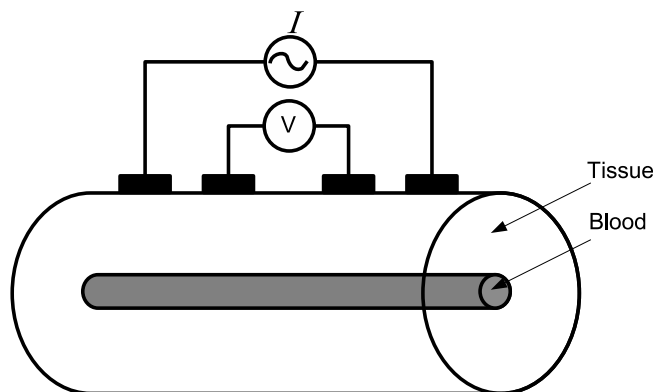


Fig. 1. A tetrapolar BIS sensor applied to a forearm model. The tetrapolar BIS sensor is composed of a pair of current injectors (outer) and a pair of voltage sensors (inner). The forearm is modelled as a cylinder which is composed of two axial compartments: blood and other tissues. The conductivity distribution is uniform in the axial direction. The former simulate volume of blood; the latter contains tissues in the forearm except for blood, *e.g.*, muscle, fat. The volume of blood increases due to blood pooling.

Blood volume is simulated as an inner cylinder and other tissues are simulated to be in the outer cylinder. Due to blood accumulation, the cross section area of the inner cylinder

increases from  $S_a$  to  $S_a + \Delta S_a$  and the impedance of this segment decreases correspondingly from  $Z_a$  to  $Z_a - \Delta Z_a$ . The fractional variation is thus  $\Delta Z_a/Z_a = -\Delta S_a/S_a$ .

There are two states for blood volume: *unconstrained*: blood volume is minimum, corresponding to impedance value  $Z_s$ ; *blood accumulated*: with an incremental volume on top of the static volume, corresponding to a lower impedance value  $Z_p$ . Based on assumption that blood pooling does not change volume of surrounding tissues, the blood pooling model of a forearm can be described as three electrical components in parallel (Figure 2).

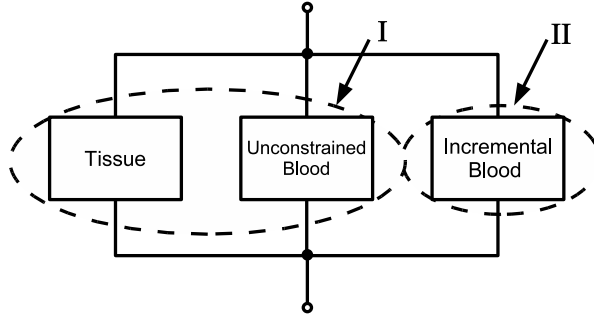


Fig. 2. In term of electrical structure, the forearm measured is modelled as three components in parallel. Tissue and static blood are grouped as part I (with impedance  $Z_I$ ), while the incremental blood is part II (with impedance  $Z_{II}$ ). During unconstrained status, the model is represented by part I; during blood pooling, the model is part I paralleled with part II due to infused blood volume.

The impedance measurements,  $Z_s$  and  $Z_p$ , originate from the tissue model (Figure 2) where tissue and static blood are represented by impedance  $Z_I$ , and incremental blood is represented by impedance  $Z_{II}$ . During static status,  $Z_s = Z_I$ , while after blood accumulation,  $Z_p = Z_I || Z_{II}$ .

Traditionally, a bioimpedance locus of a tissue can be analyzed using *Cole-Cole model*. According to Cole [6], a bioimpedance spectrum can be fitted to the Cole-Cole equation, given by (1), (illustrated as Figure 3)

$$Z_{ib}(f) = R_\infty + \frac{\Delta R}{1 + j(f/f_c)^{1-\alpha}} \quad (1)$$

where  $R_\infty$  is the resistance at infinite frequency;  $\Delta R = R_0 - R_\infty$ , where  $R_0$  is the resistance

at zero frequency;  $f_c$  is the characteristic frequency of the tissue or model under analysis; and  $\alpha$  is the constant depending on the heterogeneity of the tissue, where 0 represents completely homogeneous and 1 completely heterogeneous tissue.

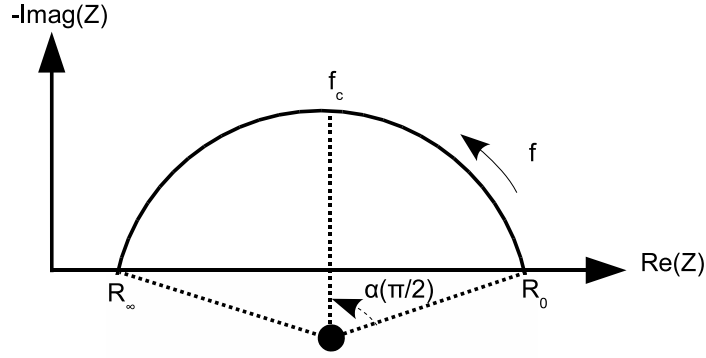


Fig. 3. Cole-Cole plot in the complex impedance plane

The Cole-Cole curve of the incremental blood (part II, in Figure 2) is calculated from two measurements: 1) the impedance spectrum  $Z_s(f) = Z_I$  before blood pooling, and 2) the impedance spectrum  $Z_p(f) = Z_I || Z_{II}$  after blood pooling. Based on these data the incremental blood impedance spectrum  $Z_{ib}(f) = Z_{II}$  is calculated by

$$Z_{ib}(f) = \frac{Z_s(f)Z_p(f)}{Z_s(f) - Z_p(f)} \quad (2)$$

which is derived from the parallel circuit illustrated by Figure 2. The calculated  $Z_{ib}(f)$  is blood-related only.

Theoretically and without noise, four independent equations are needed to calculate four Cole-Cole parameters. However, due to the data noise, solving the parameters from the theoretically minimal data set would result in large errors. It is thus necessary to use a method which calculates an approximate solution which fits the all of the measured data. In practice, Cole-Cole approximation is accomplished by curve fitting of experimental data to a semi-circular arc in the complex impedance plane, illustrated as Figure 3. In this

paper, data were fitted using the Levenberg-Marquardt (LM) algorithm [13]. The Cole-Cole model reduces a complex impedance spectrum to four parameters that can be interpreted as physical properties of the tissue under study. The resulting model parameter vector is  $m = [R_0, \Delta R, f_c, \alpha]$ .

Of the Cole-Cole parameters obtained,  $R_0$  and  $R_\infty$  are blood properties, as well as functions of body segment geometry and electrode configuration, *e.g.*, body segment geometric changes, electrode movement, and blood pressure changes; while  $f_c$  and  $\alpha$  are functions of blood properties alone. However,  $\alpha$  is known to be sensitive to variability in measurements, and relatively insensitive to variations in tissue properties, while  $f_c$  is relatively stable with respect to measurement geometry changes and more sensitive to tissue property variations [7]. This suggests that  $f_c$  is the most discriminating parameter for characterizing blood bioimpedance properties.  $R_0$ ,  $R_\infty$ ,  $\Delta R$  and the ratio  $R_0/R_\infty$  are also helpful if careful calibrations are made.

### III. METHODS: EXPERIMENTAL

In order to verify the approach presented, we conducted two experiments: the experimental phantom measurement and the equivalent circuit simulation. Their objectives were to model blood pooling behavior in the forearm and estimate the parameters of interest. A preliminary human experiment is discussed in the Section V.

#### A. Experimental Phantom

An experimental phantom was built to model the forearm structure and blood accumulation behavior (Figure 4). A piece of skinned porcine meat (size: 28 cm×14 cm×4 cm) was taken from cold storage and placed in room environment (24°C and 64% humidity) for at least six hours to reach a stable temperature in order to eliminate the temperature drift. A

groove (length= 25 cm, width=height= 2 cm) was cut at the position which was about one third of the meat width. A stick of porcine liver was cut to fill the groove. The meat base is to simulate the unconstrained status of the forearm; the porcine liver is filled to the groove to simulate infused blood after pooling.

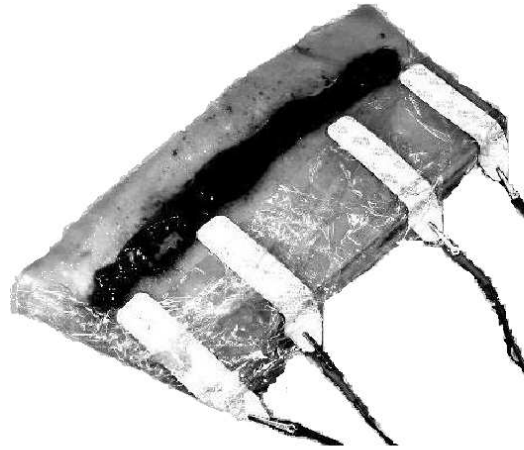


Fig. 4. Tissue phantom with a tetrapolar BIS sensor applied on the meat surface (background removed from this figure). The phantom was made of a porcine meat base, with a groove cut in it. A filling of porcine liver was filled in the groove. The meat base is to simulate the unconstrained status of the forearm; the porcine liver is filled in the groove to simulate infused blood after pooling.

The goal of this experiment was to validate the approach developed in this paper. From two sets of BIS data of the phantom (measured on meat base with and without liver filling), we estimate the bioelectrical properties of the liver. This corresponds to the model scenario: from two sets of BIS data measured on the forearm (with and without blood accumulation), we calculate the bioelectrical properties of blood.

Four skin electrodes were placed equidistantly onto the surface of the meat, illustrated as Figure 4. The inner pair were voltage sensors and the outer pair were current injectors. BIS data were collected from 5 kHz to 1 MHz (at 50 frequencies, logarithmically distributed) by an impedance analyzer (Xitron 4200 ECF-ICF Bioimpedance Analyzer, Xitron Technologies, San Diego, CA, USA).

Firstly, BIS data were measured from the isolated liver filling and Cole-Cole parameters were calculated as the standard to be compared with those of estimated. BIS data were then measured from the meat base with and without liver filling. Cole-Cole parameters were estimated from the measured data using the proposed method. Finally, estimated parameters were compared to the standard parameters obtained initially.

Three pieces of phantom base were tested and each had three liver sticks as fillings. Totally nine experiments were conducted.

### *B. Equivalent Circuit Modeling and Simulation*

A equivalent circuit model was built using electronic components (resistors, capacitors and inductors). This circuit was designed to simulate a biomaterial structure with a cylindrical model (Figure 1) based on the following geometric configuration: this model was 5cm long with a cross-section area 1cm<sup>2</sup>; it was composed of muscle (49%), fat (49%) and blood (2%), where numbers in parentheses were fractions of the cross-section area (other tissues were ignored for simplicity); blood volume increased by 10% after blood accumulation.

The dielectric properties of tissues are  $\epsilon_r(\omega)$  and  $\sigma(\omega)$ , where  $\epsilon_r$  and  $\sigma$  are relative permittivity and conductivity, respectively;  $\omega$  is the angular frequency.  $\epsilon_r(\omega)$  and  $\sigma(\omega)$  were obtained from these reported values: 1) blood (rabbit, in vitro, [14]); 2) muscle (bovine, paravertebral cut along muscle fibres, in vitro, [15]); 3) fat (human, in vitro, [15]). All dielectric data were sampled from the figures in the cited papers and interpolated along 44 points logarithmically distributed from 5 kHz to 10 MHz.

The electrical equivalent circuit of certain tissue can be represented by its conductive and capacitive components in parallel [17]. Each tissue is modelled as a RC parallel pair.

$$Y = S + j\omega C \quad (3)$$

where  $Y$  is the admittance,  $S$  is the equivalent conductance and  $C$  is the equivalent capacitance. Values of components were calculated by model geometric and dielectric properties described above, using  $C = K\varepsilon_0\varepsilon_r(\omega)$  and  $S = K\sigma(\omega)$ .  $K = A/l$  is the geometric scale where  $A$  is the tissue cross-section area and  $l$  is the finger length. At 5 kHz, the equivalent circuit of the biomaterial compartment and corresponding components values are illustrated in Figure 5.

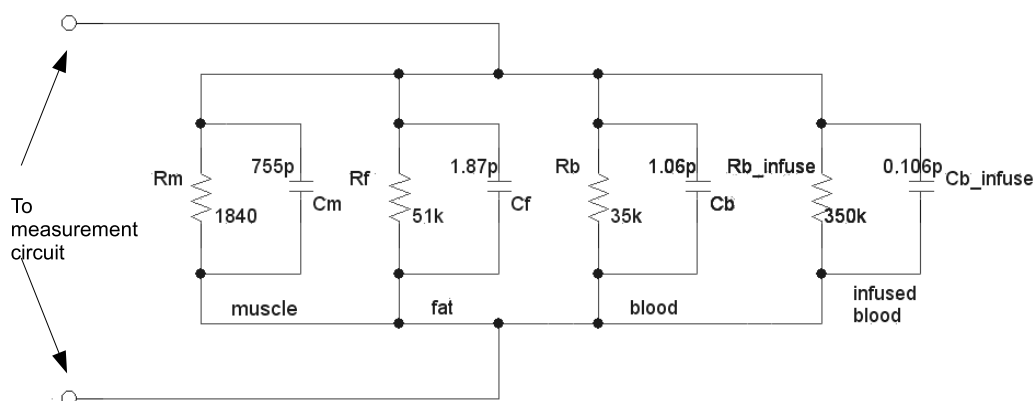


Fig. 5. units: resistors– $\Omega$ ; capacitors– $F$ . The equivalent circuit of a cylindrical biomaterial compartment is composed of muscle, fat, blood and incremental blood. Each element is approximated as an RC parallel pair. Component values were calculated from material composition, geometrical configuration and tissue dielectric properties.

## IV. RESULTS

This section presents the results of two experiments described in section III. Estimated parameters were compared with standard values, and the estimation accuracy was investigated.

### A. Experimental Phantom

Three pieces of skinned porcine meat (denoted as 1,2,3) were tested as phantom bases and each had three liver sticks as fillings (denoted as a,b,c). Results were obtained from nine experiments.

Illustrated in Figure 6(a), two BIS measurements (each was the time averaging of ten consecutive sweeps),  $Z_{base}(f)$  with and without liver filling, were made and the estimated liver BIS curve was illustrated in Figure 6(c), marked as \*. By fitting this curve using a 1<sup>st</sup> order Cole-Cole model (Figure 6(c), solid line), the liver's Cole-Cole parameters were calculated and compared with those of the previously measured original liver (Figure 6(b), time averaging of ten consecutive sweeps). After being normalized, the original and the estimated liver Cole-Cole curves were compared in Figure 6(d). The error between the original Cole-Cole model parameters  $m_0 = [R_0, \Delta R, f_c, \alpha]$  and the estimated parameters  $\hat{m} = [\hat{R}_0, \hat{\Delta R}, \hat{f}_c, \hat{\alpha}]$ , was calculated through  $e = (|\hat{m} - m_0|) ./ m_0 \times 100\%$ .

The inductive effect, illustrated as the sub-ripple at the high frequency end (Figure 6(b)6(c)), can be observed in many real measurements even on homogenous tissues [19]. In our measurements, this effect was also observed above 400 kHz. Although this additional effect could still be fitted well by using the ECFC (Extended Cole-Fricke-Cole) model [19], we chose to fit 40 frequencies (5 kHz to 339 kHz) to avoid fitting the high frequency sub-ripple, without affecting simulation results. As listed in Table I, The average parameter estimation errors ( $\mu_e$ ) of  $[R_0, \Delta R, f_c, \alpha]$  are [22.35%, 15.85%, 5.99%, 22.79%], respectively. Compared with other parameters,  $f_c$  has a much lower error level and a much narrower standard deviation.

### B. Equivalent Circuit Modeling and Simulation

According to measurements made [14],  $f_c$  of blood (rabbits, in vitro, room temperature) was about 4.132 MHz which was approximated as the frequency where the value  $f \times \epsilon_r$  was the maximum. White Gaussian noise was added into simulation data to test noise performance of the method. We defined  $nsr$  as the ratio of noise standard deviation to the amplitude of difference impedance signal. Without noise interference ( $nsr = 0$ ), the Cole-

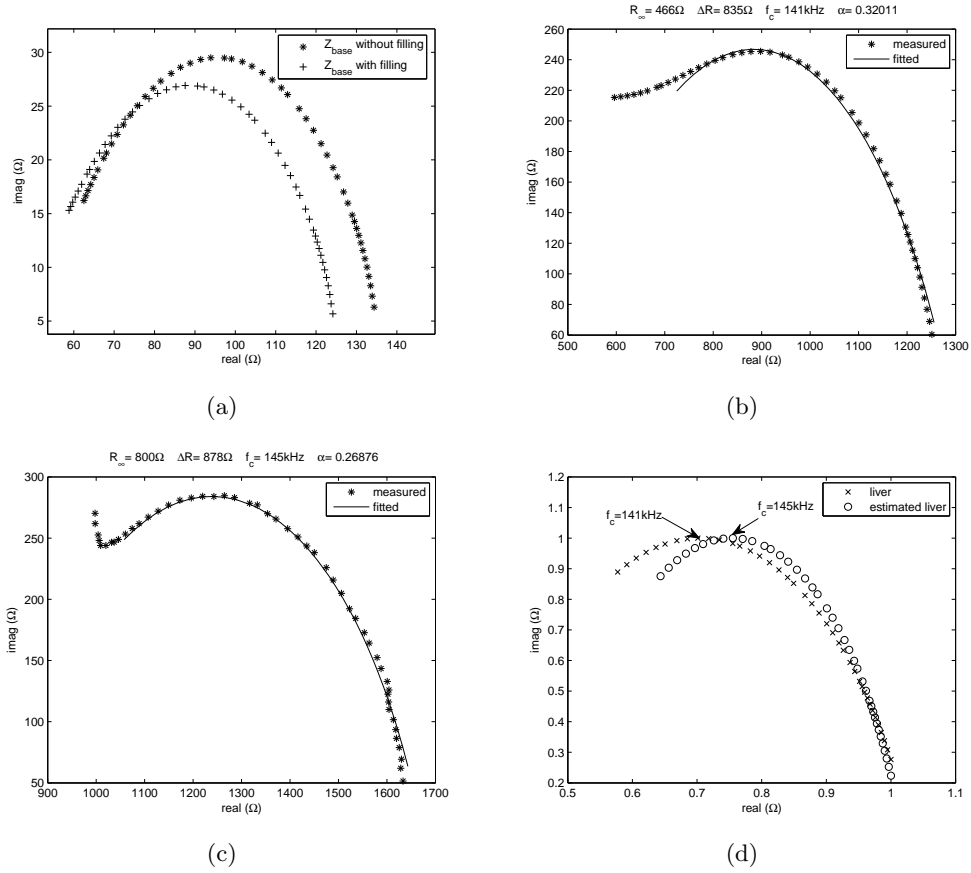


Fig. 6. A representative phantom measurement. (a) Cole-Cole curves of the meat base  $Z_{base}(f)$  without ('\*') and with ('+') liver filling; (b) The original Cole-Cole curve of porcine liver stick,  $Z_{liver}(f)$ , was fitted in a 1<sup>st</sup> order Cole-Cole model; The measurement curve and the fitted curve were represented by '\*' and solid line, respectively. (c) From data obtained in (a), the estimated Cole-Cole curve of porcine liver  $\hat{Z}_{liver}(f)$  was calculated using the proposed method. It was fitted in a 1<sup>st</sup> order Cole-Cole model. The measurement curve and the fitted curve were represented by '\*' and solid line, respectively. (d) The fitted  $Z_{liver}(f)$  ('x') and  $\hat{Z}_{liver}(f)$  ('o') were normalized.

Cole curve of blood was calculated and then fitted by a 1<sup>st</sup> order Cole-Cole model, the fitted  $\hat{f}_c$  was 4.2546 MHz with 2.97% error  $f_c$ , illustrated by Figure 7.

As noise increased, the simulated data no longer showed a consistent pattern and made curve-fitting inaccurate. Figure 8 illustrated a successful curve-fitting when  $nsr = 0.05$ . However, when the  $nsr$  was increased further, the nonlinear curve fitting could not converge to a reasonable solution. This is determined in the nonlinear curve fitting process by an

TABLE I

*Estimated ( $\hat{m}$ ) v.s Original ( $m_0$ ) Cole-Cole Parameters:*

*Measurements were made on three phantom bases (denoted as 1,2,3) and each of which had three liver sticks as fillings (denoted as a,b,c). With the smallest estimation error mean  $\mu_e$  and error standard deviation  $\delta_e$ ,  $f_c$  is a good candidate to characterize blood electrically.*

		$R_0(\Omega)$			$\Delta R(\Omega)$			$f_c(kHz)$			$\alpha$		
		$m_0$	$\hat{m}$	err(%)	$m_0$	$\hat{m}$	err(%)	$m_0$	$\hat{m}$	err(%)	$m_0$	$\hat{m}$	err(%)
1	a	1682	1530	9.04	1010	1003	0.69	157	141	10.2	0.304	0.261	14.0
	b	2086	1512	27.5	1277	1041	18.5	155	162	4.52	0.319	0.261	18.2
	c	1302	1678	28.9	835	878	5.15	140	145	3.57	0.320	0.269	15.9
2	a	1557	2076	33.3	964	943	2.18	189	157	16.9	0.301	0.251	16.7
	b	1796	1986	10.58	1185	854	27.9	149	133	10.7	0.329	0.233	29.2
	c	1369	1545	12.9	918	886	3.49	182	181	0.55	0.294	0.276	6.12
3	a	1651	1273	22.9	1455	770	47.1	149	150	0.67	0.438	0.316	27.8
	b	1535	2028	32.1	875	668	23.7	193	195	1.04	0.263	0.153	41.9
	c	2088	1590	23.9	1279	1100	14.00	155	164	5.81	0.317	0.206	35.0
$\mu_e(\%)$		22.35			15.85			5.99			22.79		
$\delta_e(\%)$		9.30			15.32			5.58			11.41		

extraordinarily large cost function value even after sufficient regression steps.

One practical approach to reduce noise is time averaging where  $nsr$  will be decreased by a factor of  $\sqrt{N}$  for independent noise, where  $N$  is the number of data sets being averaged. Figure 9 showed the normalized estimation error ( $\frac{\hat{f}_c - f_c}{f_c} \times 100\%$ ) as a function of  $nsr$  and  $N$ , where 100 independent trials were conducted and means/standard deviations were plotted in the error bar form. For low  $nsr$ , the estimation errors were below 10%, but jump dramatically when the noise exceeded a certain level, as illustrated in Figure 9.

## V. DISCUSSION

This paper introduces a method to measure differential blood impedance curve by processing bioimpedance spectroscopy data before and after blood pooling. This technique offers the advantage that the blood impedance curve is caused by a single medium, blood, while the global impedance signal is composed of all tissues lying in the field of view. Parameters (such as  $f_c$ ) of this blood curve may be more accurate for blood characterization, compared

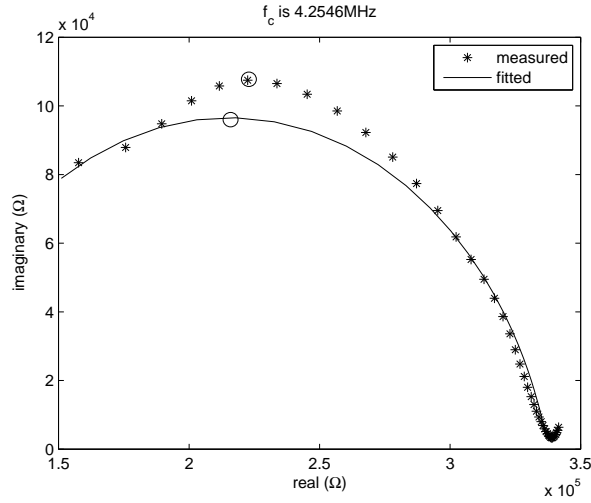


Fig. 7. Blood impedance curve calculated from circuit simulation (denoted as ‘\*’) and fitted with a 1<sup>st</sup> order Cole-Cole model (solid line). Points of  $f_c$  had been circled out on curves. The estimated  $\hat{f}_c$  was 4.2546 MHz with 2.97% deviation to the true  $f_c$ , where  $nsr = 0$ .

with those from curves such as  $Z_s(f)$  or  $Z_p(f)$  which are generated from multiple tissues due to heterogeneity in the measuring field.

To perform a preliminary *in vivo* validation of this technique, we conducted a blood pooling experiment on a human subject. A resting, healthy adult was seated with his left forearm resting on the table, the elbow approximately at the level of the heart. A tetrapolar sensor was applied on the forearm (Figure 10). The distance between two current injection electrodes was 15 cm and that of two voltage measurement sensors was 10 cm. BIS data were collected from 50 kHz to 1 MHz using the impedance analyzer (Xitron 4200 ECF-ICF Bioimpedance Analyzer, Xitron Technologies, San Diego, CA, USA). A cuff from a blood pressure meter was applied to the upper arm. The first BIS data set was measured before blood pooling (Figure 11(a), ‘\*’) and then the cuff pressure was increased to 100 mmHg which was between the normal systolic pressure and diastole pressure. This enabled the blood pooling which let arterial blood flow into the forearm but prevented venous return. The second BIS measurement was conducted after fifteen seconds of blood pooling (Figure

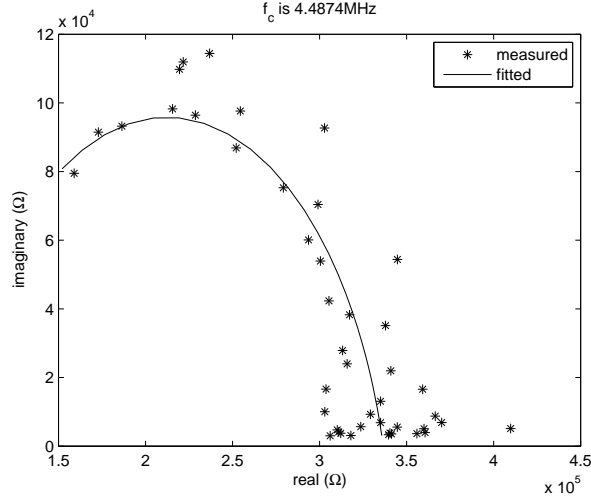


Fig. 8. Blood impedance curve calculated from circuit model with  $nsr = 0.05$  (denoted as ‘\*’) and fitted with a 1<sup>st</sup> order Cole-Cole model (solid line). The estimated  $\hat{f}_c$  was 4.4874 MHz, 8.60% deviation to the true  $f_c$ .

11(a), ‘+’). Blood spectroscopic values were calculated from those data using the method proposed in this paper (Figure 11(b)). There are clear differences between the impedance magnitudes in the human experiment (Figure 11) and the equivalent circuit simulation (Figure 7). These differences arise from the different geometries: compared with the volunteer’s forearm, the simulation is geometrically thinner (inter-electrode distance of 5 cm with cross-section area of  $1\text{cm}^2$  for the model vs 10 cm and approximately  $100\text{cm}^2$ , respectively, for the arm). Additionally, the dielectric tissue properties and blood/body fraction in the arm are unknown, and differ from the model.

The characteristic frequency of human blood is about  $1 \sim 3$  MHz [18] [8] [16]. The impedance analyzer we used (Xitron 4200 ECF-ICF Bioimpedance Analyzer) can only measure up to 1 MHz. However, given that this experiment was a preliminary exploration of the proposed technique’s *in vivo* applicability, we can obtain some useful conclusions. As illustrated in figure 11(b), the fitted curve can not show a full arc since the data measured are incomplete. Although we are not able to determine where exactly the  $f_c$  is, the BIS

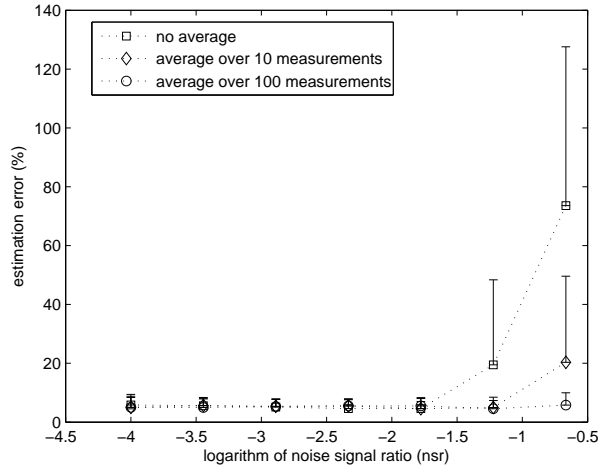


Fig. 9. The error between the estimated characteristic frequency  $\hat{f}_c$  and the true  $f_c$  is highly related to noise levels: above certain noise level, the  $\hat{f}_c$  is not a good estimate of the true  $f_c$ . However, time averaging applied on measurement data largely increases noise tolerance of the approach. Without averaging ( $\square$ ) the maximum noise level which could achieve reasonable estimations ( $\leq 10\%$ ) was  $\text{NSR} \leq 0.05$ ; with  $N = 10$  ( $\diamond$ ) and  $N = 100$  ( $\circ$ ), the maximum noise levels increased to  $\text{NSR} = 0.1$  and  $0.3$ , respectively. As illustrated, the maximum noise level which could achieve reasonable estimations ( $\leq 10\%$ ) was about 30% with time averaging on 100 measurements ( $\circ$ ), while was only about 5% for the case without time averaging ( $\square$ ).

curve of blood evidently shows that the characteristic frequency is at least 1 MHz, because the curve does not reach the highest reactance level which is specified as  $f_c$  (illustrated as Figure 3). This is consistent with previous reports ([18], [8] and [16]).

Some previous work is related to the method we propose. Yamakoshi et al. [20] showed that the changes in the admittance produced by pulsatile signal in the human finger dipped in the electrolyte vanished when the conductivity of the electrolyte was equal to that of the blood. However, this method was limited by strict experimental conditions. Brown et al. [10] tried to characterize cardiac related impedance wave measured in the chest and found inappropriate low values of  $f_c$  while comparing resulting Cole-Cole parameters with those of blood. They demonstrated that the cardiac related impedance wave was not from blood alone but a structure like “blood-tissue” parallel pair and this impedance spectrum could be misleading if used directly for blood characterization. Similar work can be found from



Fig. 10. A preliminary blood pooling experiment on human arm. A tetrapolar BIS sensor applied on the forearm. Two impedance spectroscopic curves were obtained before and after blood pooling. The upper arm is clamped by a cuff of a blood pressure meter.

Khan and Guha [21] who carried out blood pooling on a human calf to check bioelectrical variations.

In a blood pooling method such as we propose, the length of the occlusion is a key parameter. Occlusion must be long enough to provide sufficient signal (via the volume of pooled blood). However, too long occlusion results in changes in blood properties via decreased blood  $O_2$  saturation, as well as inconvenience to the subject. We selected an occlusion time of 15s as a compromise. In this paper, we show that for NSR ratios below 5%, the proposed method is able to calculate reasonably accurate estimates of the blood impedance values. In order to clarify the magnitude of acceptable noise, we first note that bioimpedance measurements are subject to noise from electromagnetic interference, electrode contact impedance, geometrical errors, movement artefacts, and instrument common mode rejection ratio (CMRR). Since this scheme proposes analysis from measurements at the same site close together in time, the electrode contact impedance and geometrical errors may be assumed to be small (since the patient may be assumed to be motionless during

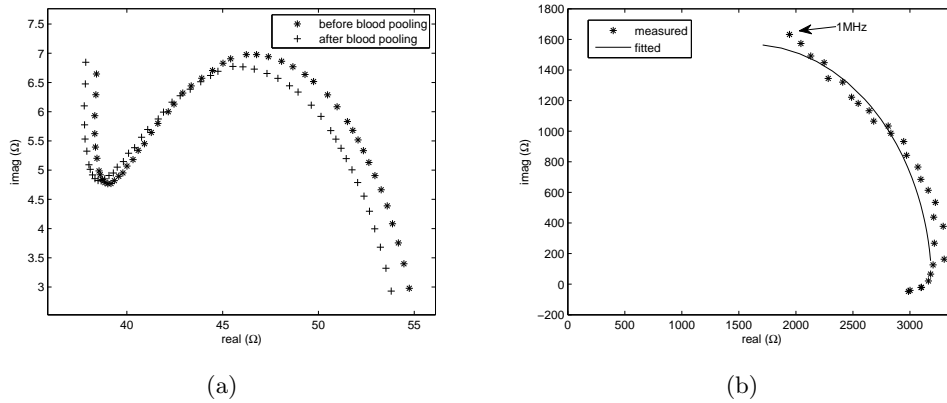


Fig. 11. The results of the preliminary human subject experiment. The data were measured from 50 kHz to 1 MHz. (a) Cole-Cole curves were measured before ('\*') and after ('+') blood pooling; (b) The Cole-Cole curve of blood, in '\*', was calculated from (a) and was fitted in a 1<sup>st</sup> order Cole-Cole model (solid line). The blood curve is not sufficient to calculate the accurate  $f_c$  due to measurement device constraint, however, it shows that the characteristic frequency is at least 1 MHz.

measurement). From the results of figure 11, measured impedance is approximately 50  $\Omega$ , and decreases by 3  $\Omega$  due to blood pooling. Considering a stimulation current 1 mA, this gives a difference signal of 3 mV with a common mode level of 50 mV. Since the electromagnetic interference signal may be reduced by averaging and use of advanced cabling, the noise is limited by the instrument CMRR, which may be considered to be about 60 dB below 10 MHz for this instrument. In this case, we estimate NSR is  $50 \times 10^{-60/20}/3 = 1.7\%$  which is well below 5%. This approximate analysis (and our preliminary human experimental results) suggests that this technique is able to achieve sufficiently low NSR levels to be practically feasible.

In conclusion, we proposed a novel scheme to calculate *in vivo* properties of blood based on measurements of the blood accumulation induced differential BIS signals. The calculated blood curve was fitted using nonlinear curve fitting method and a simple first order Cole-Cole model. Results show that  $f_c$  is a reliable parameter to characterize blood bioelectrical property *in vivo*. This method may potentially allow simplified *in vivo* measurement of blood parameters for many biomedical monitoring applications and clinical diagnoses.

## ACKNOWLEDGMENTS

This work is supported by a grant from NSERC Canada.

## REFERENCES

- [1] S. Grimnes and O.G. Martinsen, “*Bioimpedance & Bioelectricity Basics*”, San Diego, CA, USA: Academic, 2000.
- [2] M.E. Valentinuzzi, “Bioelectrical impedance techniques in medicine. part i: Bioimpedance measurement. first section: general concepts”. *Crit. Rev. in Biom. Eng.*, vol. 24, no.4–6, pp. 223–255, 1996.
- [3] S.F. Siconolfi, R.J. Gretebeck, W.W. Wong, R.A. Pietrzyk and S.S. Suire, “Assessing total body water from bioelectrical response spectroscopy”, *J. Appl. Physiol.*, vol. 82, pp. 704–710, 1997.
- [4] B.J. Thomas, B.H. Cornish and L.C. Ward, “Bioelectrical impedance analysis for measurement of body fluid volumes: A review”, *J. Clin. Eng.*, vol. 17, pp. 505–510, 1992.
- [5] J. Nyboer, *Electrical Impedance Plethymography*, (2<sup>nd</sup> ed.), Springfield, IL: Thomas, 1970.
- [6] K.S. Cole, “Permeability and impermeability of cell membranes for ions”, *Cold Spring Harbor Symp. Quant. Biol.*, vol. 8, pp. 110–122, 1940.
- [7] O. Casas, R. Bragos, R.J. Riu, J. Rosell, M. Tresanchez, M. Warren, A. Rodriguez-Sinovas, A. Carrena and J. Cinca, “In vivo and in situ ischemic tissue characterization using electrical impedance spectroscopy”, *Ann. NY Acad. Sci.*, vol. 873, pp. 51–58, 1999.
- [8] T.X. Zhao, B. Jacobson and T. Ribbe, “Triple-frequency method for measuring blood impedance”, *Physiol. Meas.*, vol. 14, pp. 145–156, 1993.
- [9] J.M. Alison and R.J. Sheppard, “Dielectric properties of human blood at microwave frequencies”, *Phys. Med. Biol.*, vol. 38, pp. 971–978, 1993.

- [10] B.H. Brown, D.C. Barber, A.H. Morice and A.D. Leathard, “Cardiac and respiratory related electrical impedance changes in the human thorax”, *IEEE Trans. Biomed. Eng.*, vol. 41, pp. 729–734, 1994.
- [11] T. Dai and A. Adler, “Blood impedance characterization from pulsatile measurements”, *Can. Conf. Computer Elec. Eng. (CCECE)*, Ottawa, Canada, May 7-10, pp. 983–986, 2006.
- [12] T.J. Ebert, J.J. Smith, J.A. Barney, D.C. Merrill and G.K. Smith, “The use of thoracic impedance for determining thoracic blood volume changes in man”, *Aviat. Space Environ. Med.*, vol. 57, pp. 49–53, 1986.
- [13] J.J. Moré, “The Levenberg-Marquardt algorithm: implementation and theory”, *Numerical Analysis*, ed. G.A. Watson, Lecture Notes in Mathematics 630, Springer Verlag, pp. 105–116, 1977.
- [14] C. Gabriel, S. Gabriel and E. Corthout, “The dielectric properties of biological tissues: I. Literature survey”, *Phys. Med. Biol.*, vol. 41, pp. 2231–2249, 1996.
- [15] S. Gabriel, R.W. Lau and C. Gabriel, “The dielectric properties of biological tissues: II. Measurements in the frequency range 10 Hz to 20 GHz”, *Phys. Med. Biol.*, vol. 41, pp. 2251–2269, 1996.
- [16] S. Gabriel, R.W. Lau and C. Gabriel, “The dielectric properties of biological tissues: III. Parametric models for the dielectric spectrum of tissues”, *Phys. Med. Biol.*, vol. 41, pp. 2271–2293, 1996.
- [17] A. Ivorra, “Bioimpedance Monitoring for physicians: an overview”, Biomedical Applications Group, CNM Barcelona, 2002.
- [18] H. Kanai, M. Haeno and K. Sakamoto, “Electrical measurement of fluid distribution in legs and arms”, *Med. Progress through Techno.*, vol. 12, pp. 159–170, 1987.

- [19] A.L. Lafargue, L.B. Cabrales and R.M. Larramendi, “Bioelectrical parameters of the whole human body obtained through bioelectrical impedance analysis”, *Bioelectromagnetics*, vol. 23, pp. 450–454, 2002.
- [20] K. Yamakoshi, H. Shimazu, T. Togawa, M. Fukuoka and H. Ito, “Non-invasive measurement of haematocrit by electrical admittance plethysmography technique”, *IEEE Trans. Biomed. Eng.*, vol. 27, pp. 156–161, 1980.
- [21] M. Khan and S.K. Guha, “Prediction of electrical impedance parameters for the simulated leg segment of an aircraft pilot under G-stress”, *Aviat. Space Environ. Med.*, vol. 73, no. 6, pp. 558–564, 2002.